Pré-Publicações do Departamento de Matemática
Universidade de Coimbra
Preprint Number 29–22

NEW PATHWAYS FOR DRUG AND GENE DELIVERY TO THE EYE: A MATHEMATICAL MODEL

J. A. FERREIRA, P. DE OLIVEIRA, P. SILVA AND R. SILVA

Abstract: Drug and gene delivery to the eye, namely to the posterior segment of the eye, is one of the most challenging problems for ophthalmologists and pharmacologists. The reason lies in the fact that the eye is protected by multiple barriers that prevent the permeation of xenobiotics and consequently prevent drugs from permeating ocular tissues. Intravitreal injection (IVI), a procedure that releases the drug directly into the vitreous, has become the gold standard for the treatment of posterior diseases. However, due to its invasiveness, several complications can occur. Medical and pharmaceutical researchers are continuously looking for new compounds, new access routes and new ways of enhancing the release. In recent years, two less invasive routes, subretinal space (SRS) and suprachoroidal space (SCS), have received considerable attention, to target the posterior segment of the eye. The aim of the paper is to present a mathematical model that simulates the coupling of an electric field with SRS or SCS injections, and to show how drug distribution compares with the gold standard, IVI. The model is represented by coupled systems of parabolic and elliptic partial differential equations. The ocular barriers are described with a certain detail. A priori estimates establish qualitative properties of the total mass released. Numerical simulations, in different scenarios, illustrate the comparative behaviour of the three treatments for short and long times. The evolution of mean drug concentration in the different ocular tissues, with and without electrical assistance, is studied.

AMS Subject Classification (2010): 35B45, 92B05, 65M60.

1. Introduction

After the brain, the eye is the most complex and specialized organ of the human body, consisting of more than two million working pieces. Apparently, the delivery of drugs to the eye - a small organ with visible access - seems an easy task but effectively it remains one of the biggest challenges of modern ophthalmology. The reason lies in the fact that multiple barriers - static, metabolic and dynamic - protect the ocular tissues. These barriers that are crucial for preserving good vision, as they prevent xenobiotics from penetrating the eye, represent simultaneously a tremendous obstacle to drug

Received October 10, 2022.

This work was partially supported by the Centre for Mathematics of the University of Coimbra-UIDB/00324/2020, funded by the Portuguese Government through FCT/MCTES.

and gene delivery (Figure 1). For these reasons the eye is one of the most inaccessible organs, in the sense that it is very difficult to achieve therapeutic concentrations in the ocular tissues.

Age related diseases of the posterior segment of the eye, as macular degeneration, diabetic retinopathy or retinal vein occlusion, attain millions of people worldwide, leading to vision impairment and blindness. As the world's population is ageing, the need for efficient approaches, based on the specific drug targeting of particular cells, is becoming increasingly urgent.

The use of mathematical models is particularly adapted to simulate innovative therapeutic approaches, in a risk-free manner. The reason of this adequacy lies in the fact that the permeation of molecules through eye tissues is a fluid dynamics problem. In fact the eye is filled with fluids: aqueous humor composed by 99% of water, in the anterior segment, and vitreous humor, a gel-like transparent fluid, in the posterior segment. These fluids play a central role in the health of the eye and coupled systems of partial differential equations are particularly suited to describe aqueous humor flow, the permeation of molecules and the action of the multiple barriers. The differential systems incorporate parameters and phenomena that regulate biological mechanisms and that can be selected as to represent healthy or pathologic situations ([1], [2], [3], [4]). To enhance the transport of molecules, physical stimuli - electrical, ultrasound or light - can be used ([5]). In the case of application of those stimuli, the fluid equations are complemented with equations representing their space-time effect.

In addition to the search for new molecular compounds, in recent years, pharmaceuticals and medical doctors have followed essentially two main complementary drug delivery strategies:

- The exploration of new possible routes for drug delivery to the anterior and posterior segments of the eye: topical, intravitreal, periocular and systemic;
- The use of minimally invasive physical forces that disrupt reversibly the protective barriers and enhance penetration: electrical fields, ultrasounds and light.

The selection of the access routes depends on the location of the tissue of the eye to be medicated. The strategy is to use the closest access, to minimize the number of barriers the drug must permeate, while taking into account

the side effects related to the degree of invasiveness. We briefly describe, in what follows, the main access routes ([1]).

Topical administration, applied locally as for example ophthalmic drops, has a very low ocular bioavailability in the anterior segment of the eye, around 5%, owing essentially to the low corneal permeability and tear turnover. However, due to its non-invasive character, it represents the most common route for administering drugs to the anterior segment of the eye. The bioavailability of topically administered drugs is even smaller in the posterior segment of the eye, with 1/100 000 of the dose penetrating the retina and the choroid. The reasons for this inefficiency lie in the long distance the drug must travel - from the cornea to the retina - and in the action of the static and dynamic barriers, it must faces ([6]).

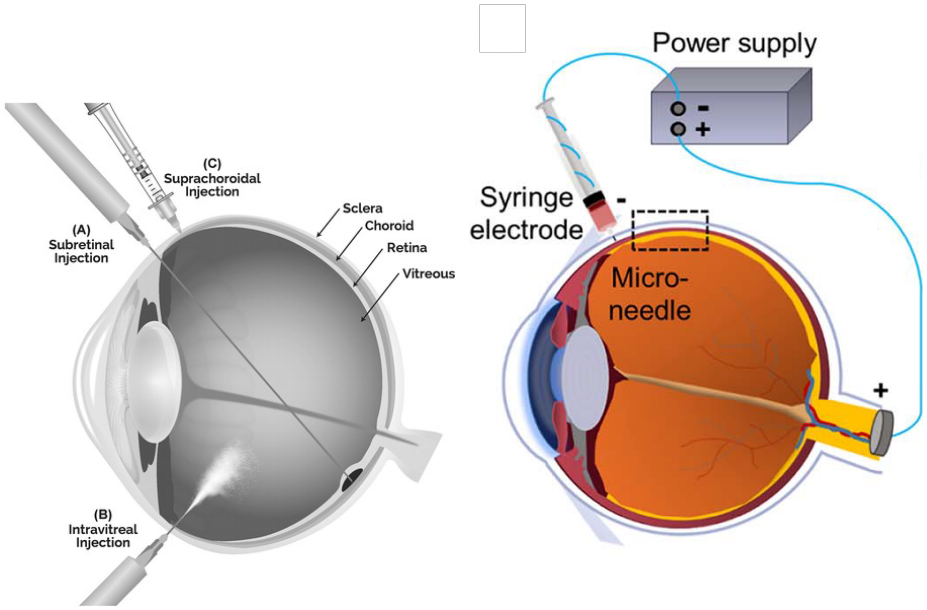

FIGURE 1. Drug administration to the anterior and posterior segment of the eye (adapted from [7]) - left and drug delivery assisted by iontophoresis. Schema of an ex-vivo procedure reprinted from [8] - right.

Systemic administration in the circulatory system has a bioavailability of less than 2% in the retina, because the inner Blood Retinal Barrier (BRB) - a restrictive barrier that regulates fluxes into and out of the retina - prevents very effectively the permeation of foreign molecules [6]. In the field of ocular drug delivery, the big challenge remains the posterior segment of the eye. As topical and systemic administration are ineffective, the idea underlying clinical research is to find alternative accesses, the closest possible to

the essential targets for posterior diseases. To target the posterior segment, different methodologies are used in clinical practice as intravitreal administration and periocular administration. The outermost layer of the retina, the Retinal Pigment Epithelium (RPE) is a very effective barrier characterized by tight junctions between its cells. In intravitreal administration - injections or implants - the molecules are released inside the vitreous, avoiding this barrier and allowing the release of high drug concentrations to the retina. For this reason intravitreal administration has become the gold standard for treatment of retinal pathologies. Nonetheless, due to its invasiveness, it can lead to serious side effects as cataract or glaucoma. In periocular administration, the molecules are released on the outer surface of the eye, in contact with the sclera. The different accesses of periocular administration are less invasive, consequently safer, than intravitreal administration. Periocular administration, facing more ocular barriers to target the retina (Figure 1), shows an important limitation due to low retinal bioavailability. A huge medical and pharmaceutical literature exists on the topic and we refer the interested reader to the review [9]. Regarding mathematical models, we mention without being exhaustive [1], [2], [3], [4] and [10].

Synthesizing, clinical researchers face the following dilemma: intravitreal administration, acting very close to the retina, achieves high bioavailability but leads to severe side effects; periocular administration acting further from the retina, is safer, but facing more ocular barriers, concentrations reached are lower. In order to achieve a compromise between efficacy and safety, scientists have directed efforts, in recent years, to release drugs in the Suprachoroidal Space (SCS) and Subretinal Space (SRS) (Figure 1). The SCS is a potential space between the choroid and the sclera, internal to the sclera and external to the choroid. The SRS is the space between the RPE cells and the photoreceptors, the first neurosensorial layer of the retina. SCS and SRS are the closest possible access gates to the retina. The proximity to the retina means avoidance of some of the ocular barriers and consequently, we can expect high bioavailability there (Figure 2). As the main target for diseases of the posterior segment of the eye is the retina, a computational study of the two new release routes and a comparison with IVI, the gold standard, assumes central importance. Suprachoroidal injections are not yet in clinical use but there is a number of clinical trials in development. Subretinal drug delivery is already being used in clinical practice.

A large number of clinical and pharmaceutical papers has addressed the problem of these new access routes. We mention for example the review [11]. Regarding mathematical models, a comparison between intravitreal delivery and suprachoroidal delivery, with no electric assistance, has been recently presented in [12].

To increase the efficiency of drug and gene delivery to target the interior layers of the retina, several researchers observe that drug bioavailability should be increased and suggest the coupling of drug delivery with the action of an electric field. The coupling of suprachoroidal or subretinal release with the action of an electric current represents one of the latest attempts to implement an efficient drug delivery procedure ([6], [8], [13]). The electric current drives the transfer of charged molecules from the SCS or the SRS into ocular tissues by temporarily weakening the barriers. In the case of delivery of low molecular weight drugs or encapsulated genes, low voltages, low intensities and exposures in the order of tens of minutes are used. The procedure is called iontophoresis. In the case of high molecular weight, high voltages pulses and intensities are used during short periods to increase, reversibly, the permeability of membranes by creating new pores. The procedure is called electroporation. We will not address electroporation in the present paper.

The model presented in this paper describes the release of small charged molecules into the SCS or the SRS, assisted by the action of an electric field, to drive the flow to the retina. To the best of our knowledge, the coupling of drug delivery from SCS or SRS, with electrical assistance, has not yet been addressed in the mathematical literature. We note that the model presented in [14] describes transscleral delivery under the action of an electric current. This paper addresses interesting aspects as for example the influence on drug distribution, of patient position after delivery. However, the action of ocular barriers, which is the main difficulty to target the posterior segment, is not taken into account. Drug delivery from SCS or SRS as well as the assistance of electric fields are under clinical trials. In clinical trials, drug concentration is measured qualitatively by indirect approaches. In fact, the primary medical outcome is the increase in visual acuity, measured by the number of letters from baseline, after a period of treatments. For this reason, mathematical models assume a central role in quantifying drug concentration *in vivo*. They provide, in a risk-free manner, a number of preliminary answers that can guide preclinical and pharmaceutical research.

In Section 2 we present the mathematical model. The physiological reasons underlying our choices are also addressed. Numerical simulations are exhibited in Section 3. In Section 4 we present a number of conclusions. A theoretical study addressing the stability of the model is included in the appendix.

2. Mathematical model

The model presented in this section can be used to describe drug release into the posterior segment of the eye, from different access gates. The model allows to analyze how the release through the less invasive accesses - SRS and SCS - assisted by iontophoresis, compares with the gold standard, IVI. Several aspects can be studied. Namely, we mention:

(1) Maximum concentration achieved in different ocular tissues and times required to attain it;
(2) Dependence of drug distribution, on electric current and application time.

The model is based on systems of parabolic and elliptic partial differential equations. The role of opthalmic barriers, that represent the main obstacles in delivering drug to the eye, is described with a certain detail. The molecules released into the SCS face the clearance of the choroidal flow, the opposition of the tightly packed cells of the RPE and the phenomenon of efflux pumps in the retina. The molecules released in the SRS avoid the RPE but face the Interior Limiting Membrane (ILM), that separates vitreous and retina, and the efflux pumps in the retina. The transport is made, in both cases, by passive diffusion and natural convection, complemented by an electrically driven convection.

The domain is composed by the vitreous chamber, the retina, the choroid and the sclera (Figure 1). The target for most pathologies of the posterior segment is the retina. We focus on the analysis of two novel access gates to the retina, that are under clinical trials or in the first clinical studies: the SCS and the SRS. We analyse drug distribution in both cases, with and without electrical assistance. As the gold standard for many retinal diseases is Intravitreal Injection (IVI), a comparison of drug concentration in the three cases is included. Although the decision of the ophthalmologist is also based on the minimization of adverse events secondary to intraocular administration, we believe that from the quantitative viewpoint our model can give useful insights.

2.1. Equations that govern drug transport assisted by an electric field. In this section we address drug delivery into the SCS and the SRS, enhanced by an electric field. Regarding electric fields there are essentially two techniques: iontophoresis and electroporation. Iontophoresis uses low voltages and low currents during tens of minutes; electroporation uses higher voltages and currents during shorter periods. The first technique is used for small molecules while the second one is adopted for large molecules as nucleic acids used in certain type of gene therapy. This last procedure is based on the application of short electrical pulses and high voltages that create new pores are formed, allowing molecules to permeate the cell membranes. We address in this paper the release of drugs with low molecular weight.

The drugs injected into the SCS or SRS are transported by passive diffusion and convection. An electric current is applied immediately after the molecules release (Figure 1). In the case of *in vivo* animal experiments, one of the electrodes is located in the syringe inserted in the SCS or SRS and the counter electrode is attached elsewhere such that the electric current can be directed to the optical nerve area ([8]). In the present paper we model the application of iontophoresis *in vivo*.

The convection field has two components: one is driven by a pressure gradient and the other by an electric potential gradient generated by the electric field. Iontophoresis employs low voltages $< 10V$, and low currents with few milliamperes, over longer periods from minutes to tens of minutes, to provide a sustained driving force. Iontophoresis acts essentially on the drug, through convection; electroporation acts not only on the drug but also on the tissues.

The different mechanisms that govern the transport in the posterior segment of the eye are described as follows (Figure 2 and Figure 3):

- Choroid (Ω_c) - Passive diffusion, convection transport, clearance due to the blood flow and permeation to the sclera and retina. The convection field has two components: one driven by a pressure gradient and the other one induced by a potential gradient.
- Sclera (Ω_s) - Passive diffusion and electric convection transport.
- Retina (Ω_r) - Passive diffusion, three component convection field - associated to a pressure gradient, to a potential gradient and to active pumping - clearance through the inner BRB, permeation through the BRB that is the RPE.

- Vitreous (Ω_v) - Passive diffusion, two component convection - associated to a pressure gradient and to a potential gradient - clearance through the hyaloid membrane and permeation to the retina through the ILM.

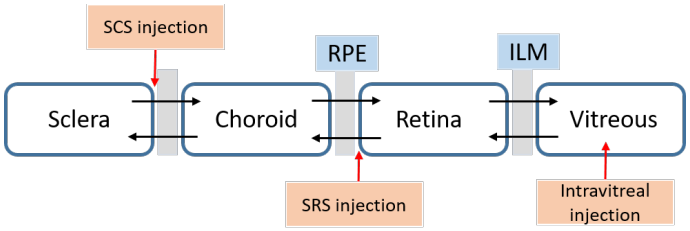

FIGURE 2. Intravitreal, SCS and SRS delivery - schema.

These phenomena are described by coupled systems of partial differential elliptic and parabolic equations, initial conditions, boundary conditions and interface conditions between adjacent regions (Figure 2). The domain, boundaries and interfaces are represented in Figure 3. The geometry is generated by taking the vitreous chamber as a circular domain with a radius of 9 mm. Thicknesses of 0.25, 0.2 and 0.4 mm are considered to represent the retina, choroid and sclera respectively. In the upper part of the domain, an ellipse was cut, to represent the boundary of the lens existing in the eyeball. Regarding the subdomains where each type of injection is applied (Ω_{inj}), their geometrical description are the following: a circumference of radius 0.2 mm for the case of intravitreal injection; a circular section of thickness 0.1 mm for SRC; a circular section of thickness 0.15 mm for SCS.

The equations that govern the concentration $c_i = s, c, r, v$, respectively in the subdomains Ω_s, Ω_c, Ω_r, Ω_v, are the following:

$$\frac{\partial c_s}{\partial t} + \nabla . J_s = q_s \text{ in } \Omega_s \times (0, T], \tag{1}$$

$$\frac{\partial c_c}{\partial t} + \nabla . J_c = -\gamma_c c_c \text{ in } \Omega_c \times (0, T], \tag{2}$$

$$\frac{\partial c_r}{\partial t} + \nabla . J_r = -\gamma_r c_r + q_r \text{ in } \Omega_r \times (0, T], \tag{3}$$

$$\frac{\partial c_v}{\partial t} + \nabla . J_v = q_v \text{ in } \Omega_v \times (0, T]. \tag{4}$$

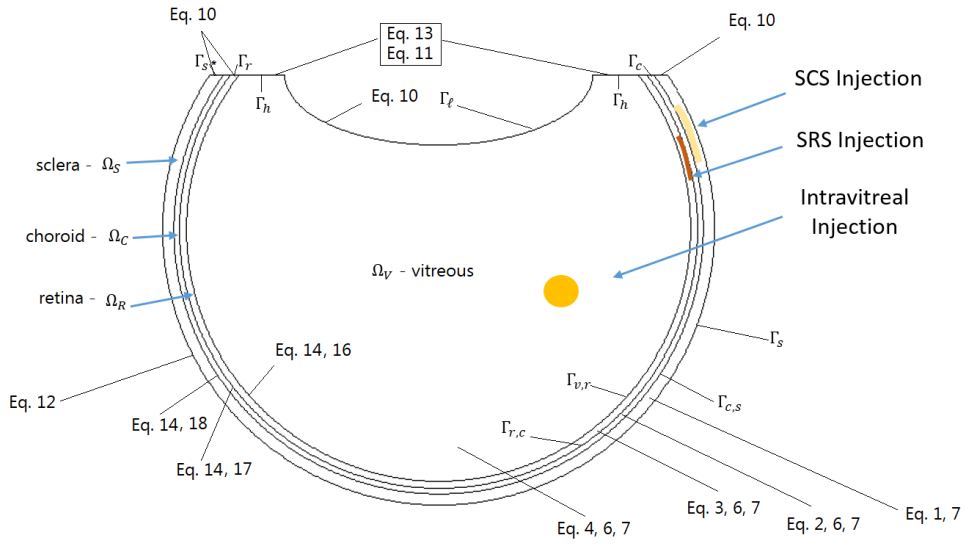

FIGURE 3. Geometry, sub-domains, boundaries and interface with main number equations.

In equations (1)-(4) the fluxes J_i, $i = s, c, r, v$, in the domains Ω_s, Ω_c, Ω_r, Ω_v, are defined by

$$\begin{aligned} J_s &= -D_s\nabla c_s - c_s u_s, \\ J_c &= -D_c\nabla c_c - c_c u_c + v_c c_c, \\ J_r &= -D_r\nabla c_r - c_r u_r + (v_r + v_r^p)c_r, \\ J_v &= -D_v\nabla c_v - c_v u_v + v_v c_v, \end{aligned} \tag{5}$$

where D_i stands for the diffusion coefficient of the drug in Ω_i, u_i represents the convection rate induced by an electric field in each subdomain Ω_i, $i = s, c, r, v$.

The convection field has one component in the sclera; two components in the choroid and the vitreous; and three components in the retina. We model the aqueous humor flow as an incompressible fluid which permeates through the porous vitreous humor according to the steady-state Darcy equation. The natural convection v_i, $i = c, r, v$, is then defined by

$$\begin{cases} v_i = -\frac{k_i}{\mu_i}\nabla p_i \text{ in } \Omega_i \times (0, T], \\ \nabla . v_i = 0 \text{ in } \Omega_i \times (0, T], \quad i = c, r, v. \end{cases} \tag{6}$$

In (6) k_i represents the permeability of the tissue and μ_i the viscosity of the fluid. The term v_r^p in the retinal flux (5) is a fictitious velocity that represents the efflux pumping phenomena, that is responsible for moving toxic substances out of the retina. In the case of intravitreal release, efflux

pumps enhance transport from the vitreous to the retina; in SCS and SRS, efflux pumps difficult the permeation of drug. The pumping in the retina could be also represented by considering different values for the inward and outward permeability in the RPE.

The second term in the right hand side of (5) represents the convection field associated with the electric potential V_i, $i = s, c, r, v$, generated by iontophoresis and is given by

$$-\nabla.(\sigma_i \nabla V_i) = 0, \qquad i = s, c, r, v. \tag{7}$$

The electric conductivity, σ_i, is assumed equal in all sub-domain, $\sigma_i = 1.13 \times 10^{-2} S/m$ ([14]). Under the action of the potencial gradient, the ions will attain a constant velocity called the drift speed u_i, $\quad i = s, c, r, v$, defined by

$$u_i = m_i \nabla V_i,$$

where m_i is the ionic mobility (m^2/Vs) and ∇V_i is the electric field. From Einstein Law ([15]) we have

$$m_i = Ze\frac{D_i}{KT}, \qquad i = s, c, r, v, \tag{8}$$

where K is the Boltzmann constant $(1.38 \times 10^{-23} m^2 kgs^{-2} K^{-1})$, T is the temperature in Kelvin degrees, Z is the valence and e the electron charge $(1.6 \times 10^{-23}\, Coulombs)$.

To simulate the release of drug into the SCS we consider the source terms $q_v = q_r = 0$ in (4) and (3), respectively. In the case of SRS delivery we assume $q_v = 0$ in (4) and $q_s = 0$ in (1). Finally to simulate intravitreal injection we assume $q_s = 0$ in (1), $q_r = 0$ in (3). The time dependent source terms q_i, $i = r, s, v$, are defined by

$$q_i(t) := \begin{cases} 0 \text{ in } \Omega_i \setminus \Omega_{inj} \times (0, T], \\ \\ \dfrac{3 \times 10^{-3}}{\sqrt{t+\epsilon}} \text{ in } \Omega_{inj} \times (0, T], \quad i = s,\ r,\ v, \end{cases} \tag{9}$$

where Ω_{inj} represents the domain where is located the source at $t = 0$.

In (9) ϵ stands for a small regularizing parameter. An analogous description for IVI has been used in [16]. The consumption terms in equations (2) and (3) are explained in the subsequent sentences, following [2]. The BRB is

composed by the inner and the outer BRB. The outer BRB is represented by the RPE. Its barrier action is described by the interface conditions presented in Section 2.2. The inner BRB is located in the inner retinal microvasculature. The inner BRB consists of retinal capillaries whose endothelial cells are linked by tight junctions. The tight junctions regulate the permeation of molecules from the blood to the retina. Its function is to feed the first two thirds of the retina. The reaction term $-\gamma_r c_r$ in (3) represents the drug clearance that occurs through the capillaries epithelium of the inner BRB. The term γ_r is defined by a piecewise function in Ω_r that takes into account the spatial distribution of the retinal capillaries that is

$$\gamma_r = \begin{cases} \gamma_{r,1} \text{ in } \Omega_{r,1} \\ \gamma_{r,2} \text{ in } \Omega_{r,2}, \end{cases}$$

with $\Omega_r = \Omega_{r,1} \cup \Omega_{r,2}$, where $\Omega_{r,1}$ is located approximately at the inner two thirds of the retina. This region is vascularized and served by the retinal blood vessels. The function γ_r in the outer one third, $\Omega_{r,2}$, is assumed equal to zero. As there is no vasculature in this domain, the definition describes accurately the action of the inner BRB.

SRS and SCS are virtual spaces. Consequently the delivery through these spaces implies their reversible enlargement for a short period of time. We observe that the change over time of SRS and SCS are not taken into account in the present model. Another aspect not included in the model, is the binding of molecules to ocular tissues. From a theoretical point of view, if binding and unbinding rates are known, the phenomenon could be explicitly introduced in equations (1)-(4) analogously to [17] or [19]. We chose not to consider the binding-unbinding phenomenon to keep the model as simple as possible, while preserving the most relevant physical processes involved.

To simplify the reading and to give a global overview of the model we present in Figure 3 a diagram indicating the equations used in each subdomain.

2.2. Barriers, boundary and interface conditions. In what follows the boundary, interface and initial conditions are defined.
Boundary conditions

- Drug concentration
  Null flux conditions on Γ_ℓ, Γ_r, Γ_c, Γ_s, (Figure 3) that is

$$\begin{cases} J_v.\eta_v = 0 \text{ on } \Gamma_\ell \times (0,T], \\ J_r.\eta_r = 0 \text{ on } \Gamma_r \times (0,T], \\ J_c.\eta_c = 0 \text{ on } \Gamma_c \times (0,T], \\ J_s.\eta_s = 0 \text{ on } \Gamma_{s*} \times (0,T]. \end{cases} \tag{10}$$

The fluxes J_i, $i = v, r, c, s$, are defined in (5). The vectors η_i, $i = v, r, c, s$, stand for the exterior unit normals to the subdomains Ω_i, $i = v, r, c, s$, respectively on Γ_ℓ, Γ_r, Γ_c, Γ_{s*}.

On the interface Γ_h, the hyaloid, that separates the posterior from the anterior chamber, we consider

$$J_v.\eta_v = A_h c_v \text{ on } \Gamma_h \times (0,T], \tag{11}$$

where A_h represents the drug transfer coefficient on Γ_h. This condition represents the loss of drug to the anterior segment.

On the exterior boundary Γ_s of the sclera, the clearance through the episcleral veins is represented by

$$J_s.\eta_s = A_s c_s \text{ on } \Gamma_s \times (0,T], \tag{12}$$

where A_s stands for the drug transfer coefficient.

- Pressure

  On the hyaloid membrane Γ_h we consider a normal intraocular pressure ([18])

$$p = 2000Pa \text{ on } \Gamma_h \times (0,T]. \tag{13}$$

Interface conditions

- Drug concentration on the interfaces $\Gamma_{v,r}$, $\Gamma_{r,c}$, $\Gamma_{c,s}$, that represent the ILM, the RPE and the membrane that divides the choroid from the sclera, respectively (Figure 3).

  We assume flux continuity and the partitioning of drug

$$\begin{cases} J_v.\eta_v = -J_r.\eta_r, \quad J_v.\eta_v = A_{v,r}(c_v - P_{r,v}c_r) \text{ on } \Gamma_{v,r} \times (0,T], \\ J_r.\eta_r = -J_c.\eta_c, \quad J_r.\eta_r = A_{r,c}(c_r - P_{c,r}c_c) \text{ on } \Gamma_{r,c} \times (0,T], \\ J_c.\eta_c = -J_s.\eta_s, \quad J_c.\eta_c = A_{c,s}(c_c - P_{s,c}c_s) \text{ on } \Gamma_{c,s} \times (0,T], \end{cases} \tag{14}$$

  where $A_{v,r}$, $A_{r,c}$, $A_{c,s}$ stand for the mass transfer coefficients and $P_{r,v}$, $P_{c,r}$, $P_{s,c}$ for the partition coefficients. In fact, the model does not consider binding. From a theoretical point of view, if binding and unbinding

rates are known, the phenomenon could be explicitly introduced in equations (1)-(4) analogously to [17] or [19]. We decided not to consider the binding-unbinding phenomenon to keep the model as simple as possible, while preserving the most relevant physical processes involved.

- Electric potential

  Regarding the electric potential we consider

$$\begin{aligned} &J_e.\eta = 0,\ J_e = -\sigma\nabla(V) \text{ on } \Gamma_{noe}, \\ &V = V_0 \text{ on } \Gamma_{in}, \\ &V = -V_0 \text{ on } \Gamma_{out}. \end{aligned} \tag{15}$$

- Pressure

  The following conditions are considered

$$\begin{aligned} &p_v = p_r,\ v_v.\eta_v = -v_r.\eta_r \text{ on } \Gamma_{v,r} \times (0,T], \\ &p_r = p_c,\ v_r.\eta_r = -v_c.\eta_c \text{ on } \Gamma_{r,c} \times (0,T], \\ &p_c = 1200Pa \text{ on } \Gamma_{c,s} \times (0,T]. \end{aligned} \tag{16}$$

Initial conditions

We assume that the injections of drug, in the vitreous, SRS or SCS, are simulated respectively by the source terms q_v, q_r or q_c, and that no drug exists elsewhere at $t = 0$, that is

$$c_i(0) = 0 \text{ in } \Omega_i,\ i = v, r, c, s. \tag{17}$$

3. Numerical Simulations

Equations (1)-(17) were solved in the geometry represented in Figure 3, using COMSOL Multiphysics software. A quadratic piecewise finite element method for the concentrations is considered. A triangular mesh automatically generated with 19990 elements is used to obtain a consistent mesh. The time integration is performed with a backward difference method, with variable order ranging between 1 and 2 and an adaptative time step.

The values used for the parameters in the numerical simulations are presented in Table I.

Table I: Value of the model parameters used in the numerical simulations.

Parameter	Value	Unit	Description	Ref
D_v	5×10^{-10}	m^2/s	drug diffusion coef. in the vitreous	[1]
D_r	3.9×10^{-11}	m^2/s	drug diffusion coef. in the retina	[1]
D_c	10^{-10}	m^2/s	drug diffusion coef. in the choroid	[1]
D_s	10^{-10}	m^2/s	drug diffusion coef. in the sclera	[1]
(k_v/μ_r)	8.4×10^{-11}	$m^2/Pa.s$	hydraulic conductivity in the vitreous	[1]
(k_r/μ_c)	2.36×10^{-15}	$m^2/Pa.s$	hydraulic conductivity in the retina	[1]
(k_c/μ)	1.5×10^{-15}	$m^2/Pa.s$	hydraulic conductivity in the choroid	[1]
$A_{v,r}$	10^{-7}	m/s	mass transfer coefficient at $\Gamma_{v,r}$	[2]
$A_{r,c}$	10^{-7}	m/s	mass transfer coefficient at $\Gamma_{r,c}$	[2]
$A_{c,s}$	10^{-6}	m/s	mass transfer coefficient at $\Gamma_{c,s}$	[2]
$P_{r,v}$	1/10		partition coefficient at $\Gamma_{v,r}$	[2]
$P_{c,r}$	1/1.33		partition coefficient at $\Gamma_{r,c}$	[2]
$P_{s,c}$	1		partition coefficient at $\Gamma_{c,s}$	[2]
A_h	10^{-7}	m/s	mass transfer coefficient at Γ_h	[1]
A_s	2×10^{-7}	m/s	mass transfer coefficient at Γ_s	[1]
$\gamma_{r,1}$	4×10^{-5}	$1/s$	drug clearance coefficient in the retina	[2]
γ_c	10^{-4}	$1/s$	drug clearance coefficient in the choroid	[2]
v_p	3.1×10^{-8}	m/s	convective pumping effect in the retina	[1]
V	2, 5	$volt$	electric potential	

Convergence tests have been carried out with meshes of decreasing size to verify that the solution is mesh independent (Table II).

Table II: Convergence tests - reference solution obtained with a mesh consisting of 65665 elements.

Number of elements	error - L_2 norm	error - L_∞ norm
3626	3.4×10^{-3}	5.7×10^{-4}
4301	2.2×10^{-3}	3.8×10^{-4}
5345	2.1×10^{-3}	3.5×10^{-4}
18661	1.8×10^{-3}	3×10^{-4}

All numerical results regarding drug distribution and mean drug concentration are represented in mol/mm^3.

3.1. Convection fields. In the vitreous, choroid and sclera the convection field has two components: one results from the pressure gradient between the hyaloid membrane and the interface choroid-sclera and the other is a consequence of the potential gradient generated by iontophoresis. In the retina there is a third convection field that represents the pumping effect ([1]).

In Figure 4 the natural velocity field is represented. Natural convection drives the aqueous humor in the vitreous body towards the retina and the mean value of the velocity norm is $6.1646 \times 10^{-9} m/s$. This value is of the same order as the one presented in [20].

In Figure 5 we exhibit the electric potential and the associated current density. The location of the active electrode containing the drug is marked with A and the region where is felt the action of the counter electrode is marked with B. Considering equation (8) the mean value of the norm of the electrical convection field is $2.4378 \times 10^{-7} m/s$.

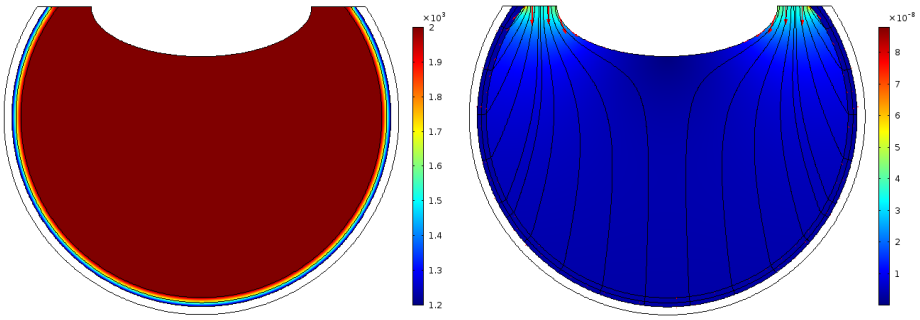

FIGURE 4. Pressure and AH path.

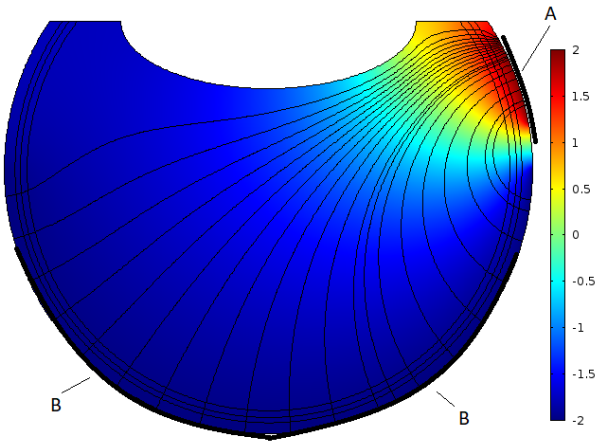

FIGURE 5. Potential and current density with $V_0 = 2$.

A positively charged drug is placed under the positive electrode. The drug is then repelled and attracted to the negative electrode. If a positive drug is released into the SCS or the SRS the convection field will point in the direction of the negative electrode. The electrode where is placed the drug

is called active electrode; the second electrode is called counter-electrode. In the animal experiments, reported in [8], related to SCS release, the counter-electrode is placed in the optical nerve, in the case of *ex vivo* laboratory tests; in the case of *in vivo* experiments, the counter-electrode is placed in the ear. If the drug is negatively charged, the drug is placed under the negative electrode and attracted to the positive one.

The direction of the electric current, described by equation (7), and the boundary conditions (15) are represented in Figure 5. We note that the mean value of the electric convection velocity is about forty times the mean value of the natural convection velocity.

3.2. The new routes and the gold standard: analysis of drug distribution. In this section we compare drug distribution after suprachoroidal, subretinal and intravitreal injection. The administration through the two new accesses - SCS and SRS - is assisted by iontophoresis. The electric field is applied during 5 minutes with a potential $V_0 = 2$.

In Figure 6 we exhibit drug distribution in the vitreous for $t = 10$ minutes and $t = 2$ hours, for the three delivery processes. As expected, higher concentrations are reached in the vitreous in the case of IVI. Regarding iontophoresis a question arises. Why we don't couple an electric field with IVI? The answer lies on the fact that drug released by IVI achieves high concentrations in the retina. This is the reason why it is considered the gold standard for retinal treatments. The attempt of pharmacologists and ophthalmologists to explore new accesses is due to the severe adverse effects of IVI.

In Figure 6 the global convection rate is composed by natural convection with order 10^{-9} m/s ([16]) plus an electric convection with order 10^{-7} m/s, while diffusion is of order 10^{-10} m^2/s. The problem is convection dominated at least during the 5 minutes that lasts electric iontophoresis.

As the main target in the posterior segment is the retina, let us define the mean drug concentration in the retina, $\bar{C}_r$, by $\bar{C}_r = \dfrac{1}{c_{r,\,max}} \displaystyle\int\int_{\Omega_r} c_r dv$.

We present in Figure 7 the evolution of $\bar{C}_r$ in the retina during 2 hours of treatment, when different type of injections are used - SCS (with and without iontophoresis), SRS (with and without iontophoresis) and intravitreal injection. It can be observed that higher concentration is achieved for the SRS injection and that iontophoresis increases concentration levels in the retina.

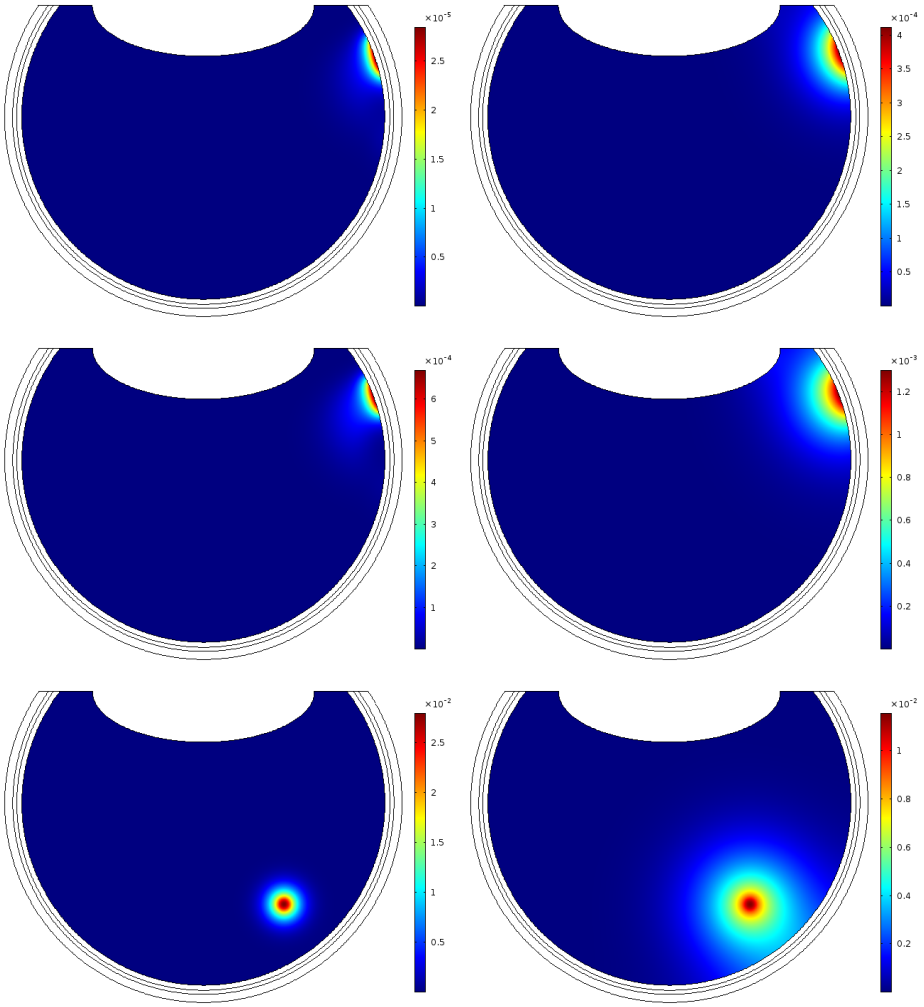

FIGURE 6. Drug concentration distribution in the vitreous for 10 minutes (left) and 2 hours (right) after administration: of a SCS injection (top), SRS injection (middle) and IVI (bottom).

To study the influence of the electric field we present in Table III, the variation of the total mass of drug released, during two hours, when iontophoresis is applied.

Table III: Effect of electric fields on the variation of mass during 2 hours.

Comparison	Vitreous	Retina	Choroid
SCS with Iont. V=2 *vs* No Iont.	25%	9,8%	2%
SRS with Iont. V=2 *vs* No Iont.	53%	17,8%	10%
SCS with Iont. V=2 *vs* Intravitreal	-99,5%	201,8%	2655%
SRS with Iont. V=2 *vs* Intravitreal	-96,1%	1221,6%	2422,3%

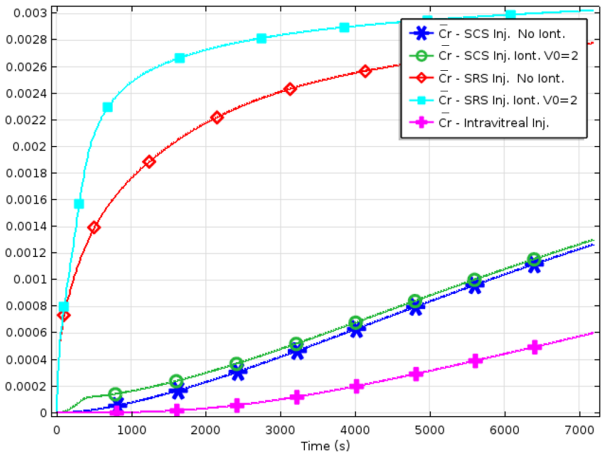

FIGURE 7. Mean drug concentration in the retina, $\bar{C}_r$, during 2 hours - comparison of SCS, SRS and intravitreal injections.

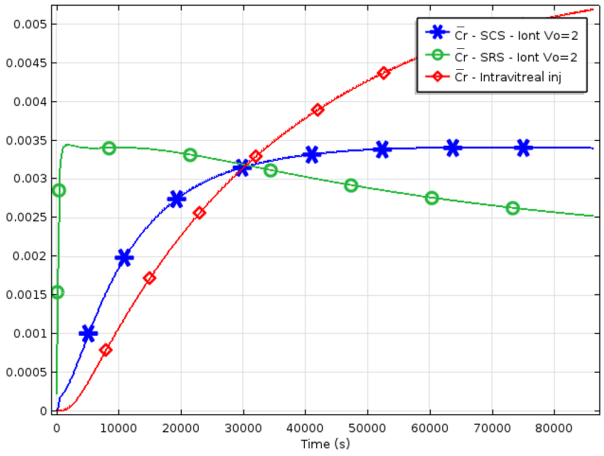

FIGURE 8. Mean drug concentration in the retina, $\bar{C}_r$, during 24 hours - comparison of SCS, SRS and intravitreal injections.

It is observed that, with the data used in the simulations, both SCS and SRS injections assisted by iontophoresis increase the mass of drug in the main tissues of the posterior segment of the eye. The greatest mass increase in the retina is achieved in the case of SRS injection. When we compare these injections with intravitreal injection, the increase of mass in the retina and the choroid is very significant.

To analyse the evolution of drug concentration for longer times, we exhibit in Figure 8 the evolution of the mean drug concentration, $\bar{C}_r$, during 24 hours. SRS and SCS injection results are obtained considering the electric field active during 5 minutes with $V_0 = 2$. Analysing the plot in Figure 8, we conclude that from the strict quantitative point of view, subretinal

delivery, coupled with electric assistance, lead to higher mean concentrations in the retina during the first 9 hours after injection. However, after this initial period, the mean concentration of drug released from an intravitreal injection achieves values four times larger than the drug delivered from SCS or SRS. These conclusions suggest that for a short time effect SRS delivery gives the best results; for a delayed effect IVI leads to the highest concentrations.

In Table IV the value of the peak concentration and the time when it is achieved for each type of injection, is presented. The drug released by IVI attains the peak concentration in the retina after 36 hours; the peaks of SCS and SRS injections are achieved after 20 hours and 0.5 hours respectively. The peak concentration of IVI is 0.0055, while the peaks achieved by SCS and SRS injections are 0.0034.

Table IV: Peak concentration in the retina and time when it is reached.

Type of administration	Peak Concentration	Time
SCS with Iont- V=2	0.0034	19.7 hours
SRS with Iont- V=2	0.0034	0.53 hours
Injection IVI	0.0055	36.7 hours

Finally, let us observe that at young ages, the vitreous has a 100% gel like structure, but at advanced ages, it is almost liquefied. The analysis of this physiological condition would imply a model of the liquefied vitreous. As a first approach, we simulate dilution, by varying the volume that the drug initially occupies in q_v, equation (9), immediately after injection. In Figure 9, we represent the evolution of the mean concentration in the retina, during 4 days for 20% and 50% reduction of the initial drug concentration. In the last case the peak concentration is 0.0028 and it is achieved after 34.7 hours. Further studies are needed to clarify the behavior of the three procedures in an aging vitreous.

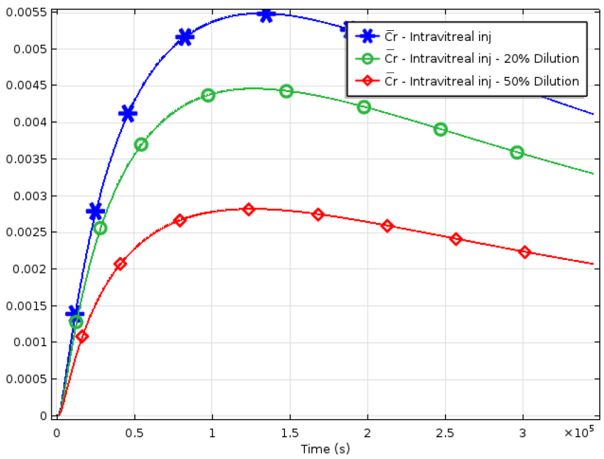

FIGURE 9. Effect of dilution of the intravitreal injection on the mean drug concentration in the retina, $\bar{C}_r$, during 4 days.

3.3. Dependence on the electric potential. In the previous sections we considered an electric field with potential $V_0 = 2$. In this section we want to analyse the dependence on V_0, of the total amount of drug released. Starting from simple protocols like the ones simulated in this article, an interesting question would be to design optimal protocols, with variable potentials and application times. An objective functional representing the drug concentration in the retina, and depending on the parameters of Table I and release periods should be defined for each delivery route.

In order to study the influence of the initial potential, we illustrate in Figure 10 the dependence of drug concentration on the electric potential, during 30 minutes and 2 hours of treatment with a SCS injection. The electric field is active during 5 minutes with $V_0 = 0, 0.25, 0.5, 1$ - left and with $V_0 = 0, 2, 5$ - right. The values used for the protocols are within the range used in laboratorial studies ([6], [12]). Increasing the entrance potential V_0, leads to an increase of the drug concentration that permeates the retina. The effect is more significant for higher voltage than for lower ones. A similar behaviour is observed for SRS injections.

To have a global picture of the whole phenomenon we analyse the effect on the different ocular tissues at $t = 1$ hour in Figure 11. The electric field acts during 5 minutes with $V_0 = 2$ and $V_0 = 5$ for the two type of injection: SCS and SRS. We note that an increase in V_0 implies a decrease of drug concentration in the sclera when a SCS injection is used. As expected in the other tissues - choroid, retina and vitreous - an increase in V_0 leads to and increase of drug concentration.

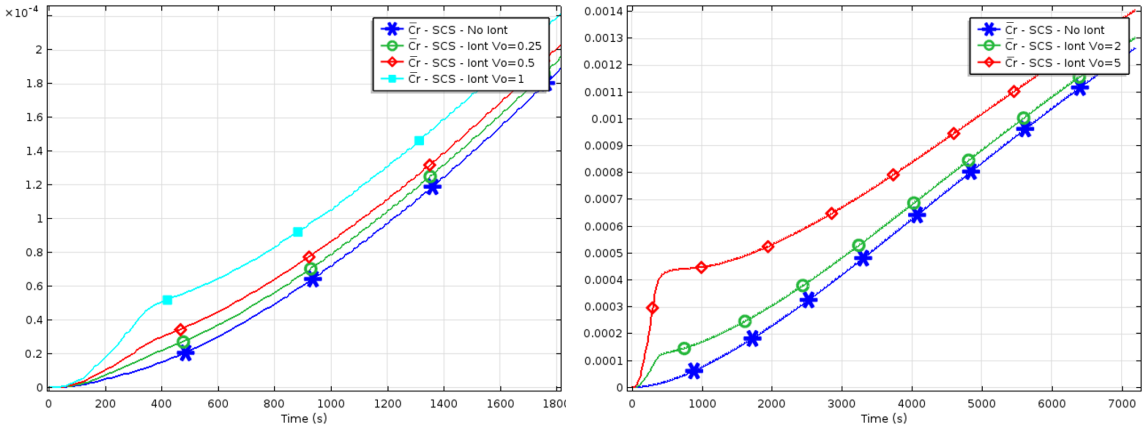

FIGURE 10. Evolution of the mean drug concentration in the retina, $\bar{C}_r$, during 30 minutes (left) and 2 hours (right) after administration of a SCS injection. The electric field acts during 5 minutes with $V_0 = 0.25$, 0.5, 1 - left and with $V_0 = 2$, 5 - right.

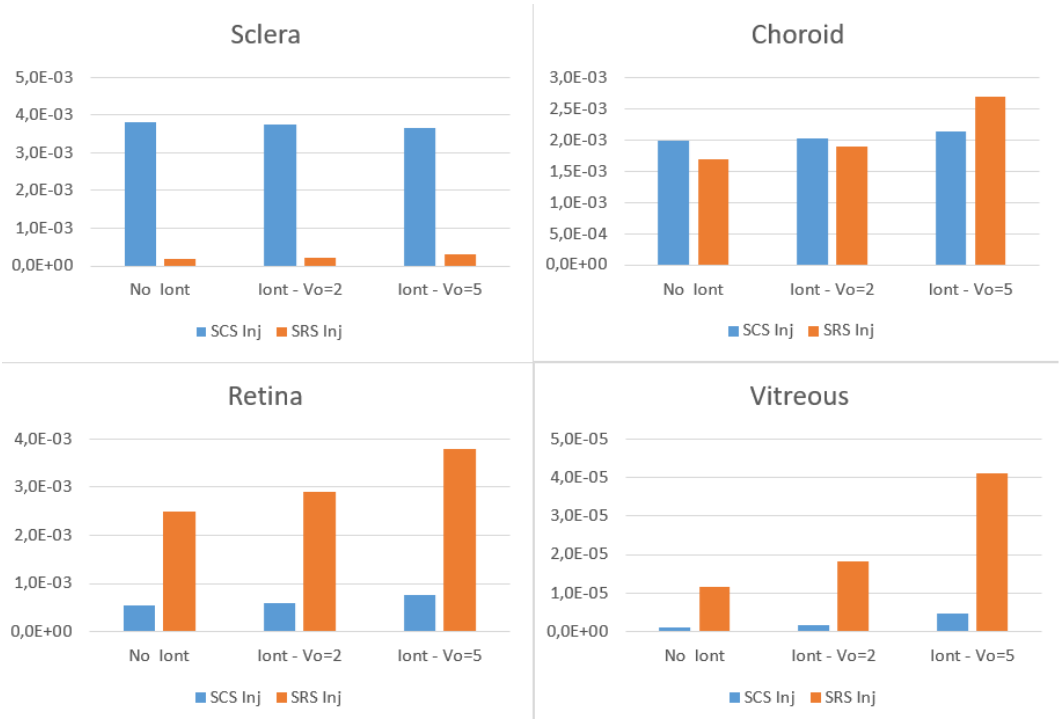

FIGURE 11. Influence of electric fields on the drug concentration in the tissues of the posterior segment of the eye at $t = 1$ hour after administration of a SCS or a SRS injection. The electric field acts during 5 minutes.

4. Conclusions

As reported in the review [21], knowledge about drug targeting to the posterior segment of the eye is still sparse and the number of clinical trials

of new drug delivery systems is reduced. A number of *in vivo* and *in vitro* models are being developed. *In vivo* animal models rise ethical concerns and introduce species differences; in the framework of *in vitro* models, human tissue is used but the living body metabolism is absent. *In silico* models can mimic ocular metabolism and associated pathologies, and consequently they represent a valuable tool to optimize new drug delivery systems, when complemented with laboratorial measurements.

Ideally, an optimal drug delivery system should exhibit a number of properties: to provide a therapeutic concentration; to be minimally invasive; and to minimize secondary effects. The mathematical model presented in this paper allows comparing three drug delivery procedures: the recent SCS and SRS injections, assisted by an electric field, with the IVI.

From a practical point of view, the model provides a number of results - for the data used in the simulations - that are synthesized in what follows:

(i) Iontophoresis enhances the amount of drug released by SCS and SRS injections in all the tissues of the posterior segment of the eye, during the first hours of drug release. (Table II);

(ii) SRS and SCS injections conjugated with iontophoresis, release a larger amount of drug during the first two hours; after this initial period, the drug released by IVI achieves larger values (Figure 10). In our simulations, the electric field is active during five minutes. The numerical results suggest that protocols, based on the use of a series of electric pulses at fixed times, can lead to an optimized SRS or SCS release;

(iii) The amount of drug released by SCS and SRS injections increases with the electric potential, in all the ocular tissues, excepting the case of SCS in the sclera (Figure 13). This can be explained by the losses through the capillaries of the choroid;

(iv) SRS injections deliver larger amounts of drug in the retina and the vitreous (Figure 13). The numerical result suggests that, in case of choroidal, retinal or vitreal disease, the option between the two novel treatments should be SRS injections;

(v) When liquefaction of the vitreous, is considered, the peak concentration of IVI is smaller and it is achieved first. The result suggests that for a liquefied vitreous - a common condition in an ageing vitreous - the amount of drug released by IVI may be substantially reduced.

We are aware that the results presented in this paper need further developments. We mention for example the study of the evolution of ocular

interfaces after SCS and SRS injections, the generalization of the model for large molecules or the design of variable voltage protocols. However, we think that the results in the present paper suggest possible pitfalls and alert to less known problems that may occur in drug release through SCS and SRS injections.

Appendix - Energy estimates

We establish in this section an energy estimate that gives *a priori* insight on the qualitative behaviour of the problem. Let Ω be a two dimensional open domain and $[0,T]$ a time interval. If w is a function such that $w : \bar{\Omega} \times [0,T] \to \mathbb{R}$ we define by $w(t) : \bar{\Omega} \to \mathbb{R}$ the function $w(t)x = w(x,t)$. Multiplying equations (1)-(4) by c_i, $i = s,c,r,v$, respectively, integrating by parts in Ω_i, summing up the four equations and taking into account interfaces conditions, we have

$$\begin{aligned}
&\frac{1}{2}\frac{d}{dt}\sum_i \|c_i(t)\|^2_{L^2(\Omega_i)} + \min_i D_i \sum_i \|\nabla c_i(t)\|^2_{[L^2(\Omega_i)]^2} + \sum_{i=c,r,v;j=s,c,r} A_{i,j}\|[c_{i,j}(t)]\|^2_{L^2(\Gamma_{i,j})} \\
&+ \sum_{i=r,c} \gamma_i \|c_i(t)\|^2_{L^2(\Omega_i)} + \sum_{i=v,s} A_i \|c_i(t)\|^2_{L^2(\Gamma_i)} \\
&\leq \sum_i \int_{\Omega_i} |w_i c_i(t).\nabla c_i(t)|dx + \int_{\Omega_v} q_v(t)c_v(t)dx.
\end{aligned} \tag{18}$$

In inequality (18) we consider an IVI procedure that is only the source q_v defined in (9) is acting. For SCS and SRS injections we take into account the sources q_s and q_r, respectively. When not stated otherwise the summation involves all the index $i = s,c,r,v$. The norm $\|.\|_{L^2(\Omega_i)}$ denotes the usual norm in the Hilbert space $L^2(\Omega_i)$ and $\|.\|_{[L^2(\Omega_i)]^2}$ represents the usual norm in $[L^2(\Omega_i)]^2$. The convection field w_i, $i = s,c,r,v$ stands for the resulting field: one component in the sclera, two components in the choroid and vitreous and three components in the retina.

In equation (18) we represent by $[c_{i,j}(t)]$ the jump discontinuity for $i = c,r,v$; $j = s,c,r$, where to simplify the presentation we have considered unitary partition coefficients. In the double index summation only the couples $(c,s)\,(r,c)$ and (v,r) are allowed (see (14)). The boundary Γ_v in the last term of the left hand side of (18) is $\Gamma_v = \Gamma_h \cup \Gamma_\ell$. Due to the null flux conditions on Γ_ℓ, only the loss through Γ_h is taken into account (11).

As

$$\int_{\Omega_i} |w_i c_i(t).\nabla c_i(t)|dx \leq \frac{1}{4\varepsilon^2}\|w_i\|_\infty^2 \|c_i(t)\|^2_{L^2(\Omega_i)} + \varepsilon^2 \|\nabla c_i(t)\|^2_{[L^2(\Omega_i)]^2}, \quad (19)$$

for all $\varepsilon \neq 0$, and

$$\int_{\Omega_v} q_v(t) c_v(t) dx \leq \frac{q_v^2(t)}{4\eta^2}|\Omega_{inj}| + \eta^2 \| \ c_v(t)\|^2_{L^2(\Omega_v)}, \quad (20)$$

for all $\eta \neq 0$, we deduce from (18)

$$\begin{aligned} &\frac{d}{dt}\|c(t)\|^2_{L^2(\Omega)} + \min_i D_i \|\nabla c(t)\|^2_{[L^2(\Omega)]^2} - \frac{\max_i \|w_i\|^2_\infty}{\min_i D_i}\|c(t)\|^2_{L^2(\Omega)} - 2\eta^2 \|c(t)\|^2_{L^2(\Omega)} \\ &\leq -2L(t) + \frac{q_v^2(t)}{2\eta^2}|\Omega_{inj}|. \end{aligned} \quad (21)$$

In (21) $\|c(t)\|^2_{L^2(\Omega)} = \sum_i \|c_i(t)\|^2_{L^2(\Omega_i)}$, $\|\nabla c(t)\|^2_{[L^2(\Omega)]^2} = \sum_i \|\nabla c_i(t)\|^2_{[L^2(\Omega_i)]^2}$ and the loss term $L(t)$ represents the sum of the three last terms of the left hand member of (18). In (21) we fixed $\varepsilon^2 = \frac{\min_i D_i}{2}$. We recall the Ω_{inj} is defined in (9) and we represent by $|\Omega_{inj}|$ its measure.

Let $k = \dfrac{\max_i \|v_i\|^2_\infty}{\min_i D_i} + 2\eta^2$. From (21) we have

$$\|c(t)\|^2_{L^2(\Omega)} \leq -\int_0^t e^{k(t-\tau)} L(\tau) d\tau + \int_0^t \frac{e^{k(t-\tau)} q_v^2(\tau)|\Omega_{inj}|}{2\eta^2} d\tau \quad (22)$$

which has a simple interpretation: the square of the norm is bounded by the balance between losses and gains in the system. The second member of (22) is continuous function of t in $[0, T]$ achieving a minimum and a maximum at least once.

If we represent by $f(t)$ this continuous function, the extrema satisfy

$$-L(t) - k\int_0^t e^{k(t-\tau)} L(\tau) d\tau + \frac{q_v^2(t)|\Omega_{inj}|}{2\eta^2} + k\int_0^t \frac{e^{k(t-\tau)} q_v^2(\tau)|\Omega_{inj}|}{2\eta^2} d\tau = 0 \quad (23)$$

Let t_M be a solution of (23). As

$$f''(t_M) = -L'(t_M) + \frac{q_v(t_M) q_v'(t_M)|\Omega_{inj}|}{\eta^2}$$

we can select η^2 such that $f''(t_M) < 0$.

In fact if $L'(t_M) > 0$ we have $\eta^2 > \dfrac{q_v(t_M)q_v'(t_M)|\Omega_{inj}|}{L'(t_M)}$ which is always verified for all $\eta \neq 0$ because $q_v'(t_M) < 0$. If $L'(t_M) < 0$ we select η^2 such that

$$\eta^2 < \frac{q_v(t_M)q_v'(t_M)|\Omega_{inj}|}{L'(t_M)},$$

and we can conclude that f attains a maximum at t_M.

Let us now search for a mininum in $[0, T]$. We have from (9) and (17)

$$\lim_{t\to 0} f'(t) = \frac{9 \times 10^{-6}|\Omega_{inj}|}{2\eta^2\varepsilon},$$

that is the concentration achieves a minimum at $t = 0$.

As the total mass released at time t, $M(t)$, satisfies

$$M(t) \leq |\Omega|\|c(t)\|_{L^2(\Omega)},$$

where $|\Omega|$ is the measure of Ω. The estimate indicates that $M(t)$ is bounded by a sectionally monotone function with a minimum at $t = 0$ and a maximum at $t = t_M$. The result in Figure 9 suggests that the same behaviour is observed for $M(t)$. An analogous result is obtained for SCS and SRS injections.

References

[1] R. K. Balachandran, V. H. Barocas, Computer modeling of drug delivery to the posterior eye: effect of active transport and loss to choroidal blood flow, Pharmaceutical Research, 25 (2008), 2685-2696.

[2] P. Causin, F. Malgaroli, Mathematical assessment of drug build-up in the posterior eye following transscleral delivery, Journal of Mathematics in Industry, 6 (2016), 9.

[3] J. A. Ferreira, P. Oliveira, P. M. Silva, R. Silva, Towards a precision ophthalmology targeting the retina, SIAM Journal on Applied Mathematics, 78 (2018), 2996-3023.

[4] J. A. Ferreira, P. Oliveira, P. M. Silva, R. Silva, Mathematics of aging: diseases of the posterior segment of the eye, Computers and Mathematics with Applications, 73 (2017), 11-26.

[5] X. Lin, X. Wu, X. Chen, B. Wang, W. Xu, Intellective and stimuli-responsive drug delivery systems in eyes, International Journal of Pharmaceutics, 602 (2021), 120591.

[6] D. Bahl, R. D. Bachu, M. Chitti, P. Chowdhury, J. Renukuntla, S. H. S. Boddu, Transscleral iontophoretic drug delivery for treating retinal diseases, Drug Delivery for the Retina and Posterior Segment Disease, (2018), 241-269.

[7] V. Kansara, L. Muya, C. Wan, T. A. Ciulla, Suprachoroidal delivery of viral and nonviral gene therapy for retinal diseases, Journal of Ocular Pharmacology and Therapeutics, 36 (2020), 384-392.

[8] J. H. Jung, B. Chiang, H. E. Grossniklaus, M. R. Prausnitz, Ocular drug delivery targeted by iontophoresis in the suprachoroidal space using a microneedle, Journal of Controlled Release, 277 (2018), 14-22.

[9] S. Raghava, M. Hammond, U.B. Kompella, Periocular routes for retinal drug delivery, Expert Opinion on Drug Delivery, 1 (2004), 99-114.

[10] M. S. Stay, L. Xu, T. W. Randolph, V. H. Barocas, Computer simulation of convective and diffusive transport of controlled-release drug in the vitreous humor, Pharmaceutical Research, 20 (2003), 96-102.
[11] R. R. Hartman, U. B. Kompella, Intravitreal, subretinal, and suprachoroidal injections: evolution of microneedles for drug delivery, Journal of Ocular Pharmacology and Therapeutics, 34 (2018), 141-153.
[12] Y. Zhang; H. Bazzazi, R. L. Silva, N. B. Pandey, J. J. Green, P. A. Campochiaro, A. S. Popel, Three-dimensional transport model for intravitreal and suprachoroidal drug injection, Investigative Ophthalmology & Visual Science, 59 (2018), 5266-5276.
[13] B. Chiang, J. H. Jun., M. R. Prausnitz, The suprachoroidal space as a route of administration to the posterior segment of the eye, Advanced Drug Delivery Reviews, 126 (2018), 58-66.
[14] J. Naghipoor, N. Jafary, T. Rabczuk, Mathematical and computational modeling of drug release from an ocular iontophoretic drug delivery device, International Journal of Heat and Mass Transfer, 123 (2018), 1035-1049.
[15] S. Gisladottir, T. Loftsson, E. Stefansson, Diffusion characteristics of vitreous humour and saline solution follow the Stokes Einstein equation, Graefe's Archive for Clinical and Experimental Ophthalmology, 247 (2009), 1677-1684.
[16] J. Kathawate, S. Acharya, Computational modeling of intravitreal drug delivery in the vitreous chamber with different vitreous substitutes, International Journal of Heat and Mass Transfer, 51 (2008), 5598-5609.
[17] J. A. Ferreira, L. Gonçalves, J. Naghipoor, P. Oliveira, T. Rabczuk, The effect of plaque eccentricity on blood hemodynamics and drug release in a stented artery, Medical Engineering and Physics, 60 (2018), 47-60.
[18] R. K. Balachandran, V. H. Barocas, Computer modeling of drug delivery to the posterior eye: effect of active transport and loss to choroidal blood flow, Pharmaceutical Research, 25 (2008), 2685-2696.
[19] S. McGinty, G. Pontrelli, On the role of specific drug binding in modelling arterial eluting stents, Journal of Mathematical Chemistry, 54 (2016), 967-976.
[20] J. Park, P. M. Bungay, R. J. Lutz, J. J. Augsburger, Evaluation of coupled convective-diffusive transport of drugs administered by intravitreal injection and controlled release implant, Journal of Controlled Release, 105 (2005), 279-295.
[21] R. V. Fernández, V. D. Tomé, A. L. Rodríguez, A. C. Penedo, X. G. Otero, A. L. Álvarez, A. F. Ferreiro, F. J. O. Espinar, Drug delivery to the posterior segment of the eye: biopharmaceutic and pharmacokinetic considerations, Pharmaceutics, 12 (2020), 269.
[22] J. Cunha-Vaz, R. Bernardes R., C. Lobo, Blood-retinal barrier, European Journal of Ophthalmology, 21 (2011), 3-9.

J. A. Ferreira
University of Coimbra, CMUC, Department of Mathematics, Coimbra, Portugal
E-mail address: ferreira@mat.uc.pt

P. de Oliveira
University of Coimbra, CMUC, Department of Mathematics, Coimbra, Portugal
E-mail address: poliveir@mat.uc.pt

P. Silva
Instituto Politécnico de Coimbra, ISEC, DFM, Rua Pedro Nunes, 3030-199 Coimbra, Portugal. CMUC.

E-mail address: pascals@isec.pt

R. Silva
University of Coimbra, Coimbra Institute for Clinical and Biomedical Research (iCBR), Faculty of Medicine, Coimbra, Portugal. Ophthalmology Department, Centro Hospitalar e Universitário de Coimbra (CHUC), Coimbra, Portugal. AIBILI - Association for Innovation and Biomedical Research on Light and Image, Coimbra, Portugal. Clinical Academic Centre of Coimbra (CACC), Faculty of Medicine; University of Coimbra, Portugal.

E-mail address: rufino.silva@oftalmologia.co.pt